RSC Advances

PAPER

View Article Online
View Journal | View Issue

Cite this: *RSC Adv.*, 2020, **10**, 10352

Preparation and evaluation of a Rubropunctatin-loaded liposome anticancer drug carrier

Dongling Xu,[a] Jiming Xie,[a] Xiaolian Feng,[a] Xiaofang Zhang,[a] Zhenzhen Ren,[a] Yunquan Zheng *[ab] and Jianming Yang *[b]

Received 11th December 2019
Accepted 23rd February 2020

DOI: 10.1039/c9ra10390b

rsc.li/rsc-advances

Rubropunctatin is a naturally occurring constituent of polyketide compounds that has great potential in the development of cancer-assisted chemotherapy. However, it has certain shortcomings such as water insolubility and photo instability that limit its clinical application. In this study, we constructed a Rubropunctatin-loaded liposome (R-Liposome) anticancer drug carrier for the first time. The results indicate that R-Liposome is water soluble, has spherical morphology, great homogeneity and dispersibility with high encapsulation efficiency (EE%, 90 ± 3.5%) and loading rate (LR%, 5.60 ± 2.5%) values. Moreover, the carrier improves the photostability, storage and pH stabilities of Rubropunctatin. The R-Liposome also prolongs the release of Rubropunctatin, enhances the anticancer activity of Rubropunctatin and encourages the mechanism of Rubropunctatin to promote apoptosis. Therefore, liposomal nanoparticles have great potential as drug delivery vehicles of Rubropunctatin for cancer treatment.

1. Introduction

Red mold rice (RMR) is produced by the cultivation of *Monascus* species on steamed rice. In China and Asia, red mold rice has been widely used as a food additive and in traditional pharmaceuticals for centuries.[1,2] Scientific evidence shows that RMR has proven to be effective for the management of cholesterol, diabetes, cardiovascular disease, and also for the prevention of cancer.[3–8] The functions of RMR can be attributed to their *Monascus* pigments. According to investigations, at present it is estimated that more than one billion people may eat products containing *Monascus* pigments during their daily lives, and the annual output of *Monascus* pigments, usually in the form of RMR, is approximately 20 000 tons in China alone.[9–11]

Monascus pigments, which belong to polyketide compounds, have proven to be toxic to various human cancer cells, indicating that *Monascus* pigments are natural non-toxic anti-tumor agents with great potential in the development of cancer-assisted chemotherapy.[12–16] Additionally, our previous study demonstrated that Rubropunctatin showed a higher anti-proliferative effect than other pigments on BGC-823 cells.[15] Moreover, the inhibitory effect of Rubropunctatin is better than that of taxol, and its toxicity towards normal human gastric epithelial cells (GES-1) is less than that of taxol.[17] In addition, the inductive effect of apoptosis was boosted by light irradiation, indicating that Rubropunctatin is a promising natural dual anti-cancer agent for photodynamic therapy and chemotherapy.[15] Its potent anti-cancer activity makes Rubropunctatin a potential anti-cancer drug. However, its clinical application has been greatly limited due to its water insolubility and light instability as the active ingredient of hydrophobic drugs cannot be dissolved before it is available for absorption in the gastrointestinal tract.[18] Therefore, improving the bioavailability of Rubropunctatin, including improving its water solubility, stability and intestinal permeability, is the main emphasis of our research.

So far, numerous studies have reported the use of various drug delivery systems such as polymers,[19] dendrimers,[20] and liposomes[21–23] to enhance water solubility and the therapeutic efficacy of lipophilic drugs. Our group has already carried out work towards cyclodextrin embedding in the early stage,[18] but cyclodextrin has poor water solubility and unfavorable nephrotoxicity, and cannot be used in liquid preparations. Liposomes are well-studied nanocarriers due to their ability to entrap both hydrophilic and lipophilic compounds, and due to their biocompatibility properties. A number of biologically active, lipophilic, and natural product-derived compounds have also been extensively studied for their anti-cancer activities in the form of liposome nanoparticles, such as paclitaxel, curcumin,[24] and camptothecin.[25] A large number of liposome-based drugs have obtained FDA-approval for cancer treatment and a number of them are currently being investigated in clinical trials (phases I–III).[26,27] Liposomes are, consequently, promising nanocarriers that could be utilized to improve water solubility, bioavailability, and the anti-cancer properties of

[a]*College of Chemistry, Fuzhou University, 2 Xueyuan Road, Fuzhou, Fujian 350116, China. E-mail: yunquanzheng@fzu.edu.cn*

[b]*Fujian Key Laboratory of Medical Instrument and Pharmaceutical Technology, Fuzhou University, 2 Xueyuan Road, Fuzhou 350116, China. E-mail: jmyang@fzu.edu.cn*

Rubropunctatin. Moreover, to our knowledge, the anti-cancer activity of Rubropunctatin in the form of nanoparticles with liposomes has not yet been evaluated.

2. Materials and method

2.1 Materials

Monascus azaphilone, Rubropunctatin, was purified in our laboratory. Cervical adenocarcinoma HeLa cells were purchased from the Cell Resource Center of the Shanghai Biological Sciences Institute (Chinese Academy of Sciences, Shanghai, China). Fetal bovine serum (FBS) was obtained from Invitrogen GmbH (Karlsruhe, Germany). DMEM medium was obtained from Gibco BRL (Gaithersburg, MD, USA). Gentamicin, L-glutamine and 1,3-diphenylisobenzofuran were purchased from Sigma (St. Louis, MO, USA). PBS (pH 7.2) was obtained from Shanghai Yuanpei Biotechnology Co. Ltd. (Shanghai, China). All solvents used were of analytical grade and the obtained Annexin-V/PI staining kits were purchased from KGI Biotechnology Development Co., Ltd. (Nanjing, China). Soybean lecithin and cholesterol were purchased from Shanghai Yuanye Biotechnology Co. Ltd and Shanghai Maikelin Biotechnology Co. Ltd, respectively.

2.2 UV-vis analysis

The concentration of Rubropunctatin in formulations was determined using a UV-vis spectrophotometer. Stock solutions of Rubropunctatin (1 mg mL^{-1}) were prepared in methanol. The Rubropunctatin stock solution was then diluted to obtain final concentrations of 12.5, 10.0, 9.0, 7.2 and 3.6 μg mL^{-1}. The mixture was then sonicated for 10 min. After being fully dissolved, 1 mg mL^{-1} of the Rubropunctatin–methanol solution was obtained for full wavelength scanning. After 40 times dilution, the full wavelength of the Rubropunctatin methanol solution was scanned between 300 and 800 nm. The maximum absorption wavelength of the Rubropunctatin–methanol solution was 467 nm. Moreover, a blank liposome dissolved in methanol had no absorption at 467 nm. Therefore, the absorbance was measured at 467 nm. The absorption value of the standard solution was measured at 467 nm. The Rubropunctatin concentration was calculated using the following formula:

$$A = 0.07533C - 0.16812,\ R^2 = 0.9956 \quad (1)$$

where (A) is the absorbance value and (C) is the Rubropunctatin concentration.

2.3 Cell culture

Human cervical cancer HeLa cells were grown in DMEM medium, 10% (v/v) FBS 40 units per mL gentamicin and 20 mmol L^{-1} L-glutamine were supplemented. Then the HeLa cells were incubated in a 37 °C humidified incubator containing 5% CO_2 (Series 8000WJ, Thermo Scientific, USA). The medium was replenished every other day and the cells were sub-cultured after reaching equilibrium.

2.4 Preparation of the liposomal suspension

A blank liposome was obtained using a thin film evaporation method, followed by sonication. 0.0144 g of soybean lecithin and 0.0072 g of cholesterol were precisely weighed and placed in a 100 mL pear-shaped bottle, and then 10 mL of CCl_4 was slowly dripped into the mixture. The solvent was evaporated with a rotary evaporator at 40 °C to form a thin film of dry lipid on the wall of the flask. The film was then hydrated by adding 30 mL of phosphate buffer solution (PBS, pH 7.2) for 3 h to form multilamellar vesicles (MLV). Ultimately, the small unilamellar vesicles (SUV) were formed from the MLV by ultrasonication (100 W, 10 min) and were stored at 4 °C.

The same procedure was applied to prepare the Rubropunctatin-loaded liposomes (R-Liposomes) except that, in this case, the organic phase contained 1 mL Rubropunctatin acetone solution (1 mg mL^{-1}).

2.5 Transmission scanning electron microscopy

The morphology of the R-Liposome was examined using transmission electron microscopy (TEM). A drop of dispersed liposome was stratified onto a carbon coated grid and left to adhere onto the carbon substrate for about 30 min. The excess was removed, and phosphotungstic acid hydrate (2%) was added. After drying, the grid was observed using TEM (JEM-200 CX, JEOL, Japan).

2.6 Measurement of particle size and potential

The particle size (PS) is one of the most important characteristics affecting the *in vivo* fate of micelles and also for determining the rate and extent of drug release.[28] The polydispersity index (PDI) is used to measure the heterogeneity of the diameter of molecules or particles in a mixture.[29] Both PS and PDI values of R-Liposome were measured in triplicate by dynamic light scattering using a Malvern system (ZEN-3600, Malvern Instruments, Worcestershire, UK) at 25 °C. The R-Liposome suspension was diluted with distilled water at the ratio of 1 : 40 (v : v) to obtain a solution with uniform scattering intensity, and this then underwent ultrasonication for 5 min. Each sample was measured in triplicate.

2.7 Study on the encapsulation efficiency and loading rate

Determination of the entrapment efficiency (EE%) and loading rate (LR%) of the liposome occurred using Sephadex column chromatography. The concentration was then determined by a UV-vis spectrophotometer. 6 g SephadexG-50 was soaked in distilled water for 24 h, then washed several times and the supernatant was removed, and ultrasonic bubbles were discharged. The above treated SephadexG-50 was then placed into a glass column (1.5Φ × 20 cm) to a suitable height. The gel column was equilibrated with distilled water.

Then, 0.5 mL of R-Liposome was added to the gel column, distilled water was eluted, and the flow rate was 0.5 mL min^{-1}. The eluent (1 mL pertube) was collected. The absorbance value of each eluent was measured at 430 nm wavelength (the

maximum absorption wavelength of the R-Liposome suspension in distilled water), and elution curves were drawn.

0.5 mL R-Liposome was added into the gel column precisely and was eluted with distilled water. 10 mL R-Liposome suspension effluent was collected. 2.5 mL of the effluent samples was mixed with 2.5 mL methanol. The absorption was measured at 467 nm. According to the standard curve of Rubropunctatin, the total amount of Rubropunctatin encapsulated in 0.5 mL of R-Liposome suspension (m_1) was obtained.

In addition, 0.5 mL of methanol was added to 0.5 mL of the R-Liposome suspension, and was then ultrasonicated for 5 min. The absorbance of the demulsified samples was measured at 467 nm. According to the standard curve of Rubropunctatin, the total amount of Rubropunctatin in the sample R-Liposome suspension (m_0) was calculated, and the EE% and LR% of the R-Liposome suspension were calculated using the following formulas:

$$\mathrm{EE}\% = \frac{m_1(\mu g)}{m_0(\mu g)} \times 100\% \quad (2)$$

$$\mathrm{LR}\% = \frac{m_1(\mu g)}{m_2(\mu g)} \times 100\% \quad (3)$$

where m_0 corresponds to the total Rubropunctatin, m_1 corresponds to the Rubropunctatin encapsulated in liposomes and m_2 corresponds to the weight of the liposomes.

Three batches of R-Liposome suspensions were taken and the process was repeated three times according to the above steps to determine the EE% and LR% of the suspensions.

2.8 Study into the photostability

To analyze the photostability, Rubropunctatin (1.0 mg mL^{-1}) and R-Liposome were exposed to a tungsten lamp (500 W, wavelength: 597–622 nm). 100 μL R-Liposome was dissolved in 3.9 mL of 80% absolute ethanol solution. Then, the samples were exposed to a tungsten lamp. The irradiation was stopped at different time intervals (0, 0.5, 1, 1.5, 2, 3, and 4 h) to detect the concentration of absorbance with a UV-vis spectrophotometer. Under the same conditions, the control group of Rubropunctatin was set. The storage rate of Rubropunctatin was calculated at different times to evaluate its stability.

The preservation rate of the Rubropunctatin and R-Liposome was calculated as follows:

$$\text{Preservation rate} = A_x/A_0 \times 100\% \quad (4)$$

where A_x refers to the absorbance of the sample after processing and A_0 is the absorbance value for the samples that have not been specifically treated.

2.9 *In Vitro* drug release

The *in vitro* release of Rubropunctatin from R-Liposome was assessed in PBS using dialysis bags (MW: 500). 3 mL from the liposomal preparation was placed in a dialysis bag. Then, the dialysis bag was placed in a beaker containing 40 mL PBS (containing 0.1% Tween80, pH 7.2). The function of Tween80 was to increase the solubility of free Rubropunctatin in PBS. The samples were mixed in a water bath at 37 ± 0.5 °C and the dialysate was stirred at 100 rpm. 2 mL was withdrawn from the dialysis bag at the specified times (0, 0.5, 1.5, 2, 3, 4, 5, 6, 7, 8, 10, 12, 24 and 48 h) and analyzed by UV-vis spectrophotometry at 470 nm (maximum absorption peak position of Rubropunctatin dissolved in PBS), as described previously. At the same time, 2 mL of fresh PBS release medium containing 0.1% Tween80 was added.

The cumulative release rate of Rubropunctatin was calculated using eqn (2)–(5).

The cumulative release rate%

$$= \left(V_0 \sum_{1}^{n-1} C_i + V_1 C_n / m_0 \right) \times 100\% \quad (5)$$

Among them, V_0: the volume of each sample, 2.0 mL; V_1: total volume of release medium, 40 mL; C_i: the concentration of Rubropunctatin at the first sampling in μg mL^{-1}. m_0: the total amount of Rubropunctatin in the sample; n: sampling times.

2.10 Cytotoxicity assay

The *in vitro* cytotoxic effect of R-Liposome was demonstrated with HeLa cells *via* an MTT assay. Cells (1×10^4 per cell) were seeded in 100 μL of medium into sterile 96-well plates. After 24 h of incubation, the medium in the 96-well plates was discarded and replaced with 100 μL of medium that contained the tested components at final concentrations of 0, 10, 25, 50, 75, and 100 μmol L^{-1}, each replicated six times. These plates were then incubated in a 37 °C humidified incubator with 5% CO_2 for 24 h. The medium was then discarded and replaced with 100 μL of MTT solution (0.5 mg mL^{-1}). The culture was then incubated for 4 h at 37 °C. Afterwards, the supernatant was removed and 100 μL of DMSO was added to dissolve the blue formazan. The optical density (OD) was determined at 570 nm. The percentage of inhibition was calculated using the following formula:

$$\text{Growth inhibition (\%)} = 1 - (\mathrm{OD_{test}}/\mathrm{OD_{control}}) \times 100\% \quad (6)$$

2.11 Cell apoptosis assay

The effect of R-Liposome on the apoptosis of HeLa cells was performed with the Annexin V/PI assay. Cells (1.0×10^5 HeLa cells per well) in the logarithmic growth phase were seeded into 6-well plates. Then, the cells were cultured in incubation at 37 °C and 5% CO_2. After 24 h of incubation, the culture medium was discarded and the cells were washed twice with PBS. A serum-free medium containing different concentrations of R-Liposome (0, 10, 25, 50, 75, and 100 μmol L^{-1}) was added and the cells were incubated for 24 h. The supernatant of each pore was collected and centrifuged (2000 rpm, 5 min) to collect the suspended cells. Adherent cells were digested by trypsin without EDTA for 1 min and centrifuged to collect the suspended cells corresponding to each pore. Then, the cells were

washed twice with PBS and collected by centrifugation. Each sample was added to 500 μL od binding buffer suspension cells. The cells mixed with 5 μL Annexin V-FITC, and 5 μL PI was then added to the mix, evenly. Afterwards, after reacting for 10 min at room temperature and under light shielding, the stained cells were analyzed by flow cytometry.

2.12 Statistical analysis

All data were expressed as the mean ± SD from the three independent experiments. Statistical analysis was performed using SPSS 17.0 software, origin 9.0 and prism 5.0. Group differences were assessed by student's *t* test, and were considered significant for $p < 0.05$ (*) and $p < 0.001$ (***).

3. Results and discussion

3.1 Characterization of R-Liposomes

As shown in Fig. 1A(i), the free Rubropunctatin was clearly water insoluble. Images of the water solution of blank liposome (Fig. 1A(ii)) featuring a milky white liquid and R-Liposome (Fig. 1A(iii)) featuring a uniform, dispersed dark brown liquid were observed. It could be concluded that the solubility of the R-Liposome was significantly increased.

In Table 1, the blank liposome had a mean size distribution of 187.8 ± 0.6 nm with a good PDI value (0.327 ± 0.014),[30] indicating that the prepared liposome belongs to a large single-chamber liposome (the particle size distribution is between 100 nm and 1 μm). After encapsulating the Rubropunctatin, the mean diameter of the liposome was 205.4 ± 1.2 nm with an acceptable PDI of 0.361 ± 0.021 and a zeta potential of 61.8 ± 0.9 mV. In addition, we can see from Fig. 2A and B that both the blank liposome and the R-Liposome have narrow monodispersed unimodal size distribution patterns, indicating that they have uniform size. The zeta potential and PDI are two of the indicators of the surface charge of the nanoparticles. It has been reported that a higher zeta potential (>|30 mV|) indicates that the particles in the suspension prevent particle aggregation due to mutual repulsive forces, thus interparticle aggregation can be avoided, and the stability can be maintained for a long period of time.[31–33] Therefore, the results indicate that R-Liposome has good stability, which is in agreement with the results determined using TEM. It can be seen from Fig. 1B that the R-Liposome consists of spherical or nearly spherical closed vesicles. These vesicles have a bilayer structure with a particle size of about 200 nm, a relatively uniform size and good dispersibility. The results indicate that the R-Liposome system has great homogeneity and dispersibility.

After 3 months in storage at room temperature in the dark, the particle size of the R-Liposome suspension did not change significantly ($p < 0.05$), indicating that the prepared R-Liposome suspension has good stability and can be kept for at least this period of time.

The R-Liposome suspension eluted at 4 mL of the effluent and was fully collected at 13 mL (Fig. 2C), indicating that the hydrophobic unencapsulated Rubropunctatin was not eluted, and that the method could separate R-Liposome and unencapsulated Rubropunctatin successfully. It could be concluded that the R-Liposome we prepared has a high EE% (90 ± 3.5%) with an acceptable LR% (5.60 ± 2.5%) (Table 1).

In conclusion, the particle size, PDI, zeta potential, EE%, and LR% data clearly show the formation of R-Liposome with better solubility and stability.

3.2 pH stability

According to a previous study, Rubropunctatin remained stable in a solution environment with pH < 5.7.[34] At pH > 5.7, the Rubropunctatin undergoes a reversible reaction, producing a compound that is insoluble in alcohol.

As shown in Fig. 3A, the characteristic absorption peaks and peak types of Rubropunctatin changed with different degrees of pH value. As can be seen from the figure, the absorbance of the solution increased as the pH value of the environment increased. It is known that the pH of the solution had a great influence on the structure of Rubropunctatin.[17] Thus, it was speculated that when the solution is alkaline, the intracellular ester group of Rubropunctatin is hydrolyzed, generating the –COOK and –OH, thereby increasing the solubility of the pigment molecules, resulting in an increase in the maximum absorbance of the dye solution and a change in the peak shape of the characteristic absorption peak.

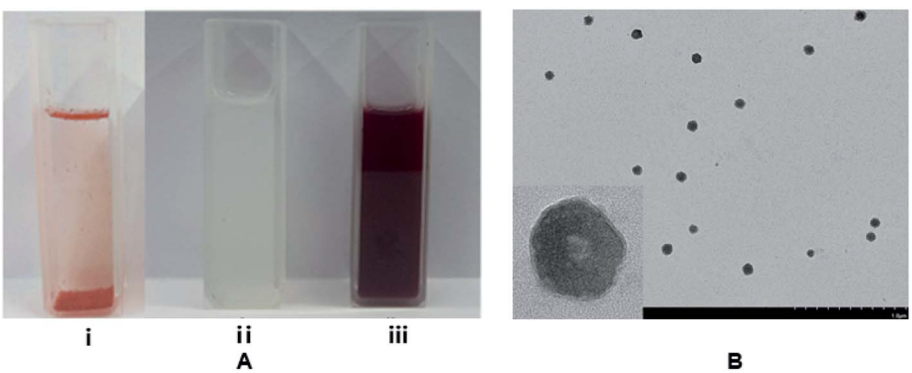

Fig. 1 (A) Water solution of Rubropunctatin (i), blank liposome (ii) and the R-Liposome suspension (iii); (B) TEM image of R-Liposome.

Table 1 Physicochemical properties of the blank liposome and R-Liposome

	PS (nm)	PDI	Zeta potential (mV)	EE (%)	LR (%)
Blank liposome	187.8 ± 0.6	0.327 ± 0.014	−58.5 ± 1.4	—	—
R-liposome	205.4 ± 1.2	0.361 ± 0.021	−61.8 ± 0.9	90 ± 3.5	5.6 ± 2.5

As shown in Fig. 3B, when the pH of the solution is 3–11, the UV-visible spectrum of the R-Liposome suspension did not change much, and the absorbance at the maximum absorption peak at 430 nm was 0.789 ± 0.009, indicating that the R-Liposome suspension had relatively good stability in this pH range. When the pH of the solution was 2.0 and 12.0, the UV-vis spectrum of the suspension was observed to change, and the absorbance at the maximum absorption peak decreased (A_{430} was 0.719 at pH 2.0; A_{430} was 0.733 at pH 12.0). At this point, due to the extreme acidity and alkalinity, part of the phosphatidylcholine in the liposome undergoes a hydrolysis reaction in a short period of time, resulting in a decrease in the concentration of the R-Liposome suspension.

In conclusion, the R-Liposome suspension did not cause solution absorption in an alkaline environment. The increase in value, before and after the comparison, showed that the Rubropunctatin molecule in the R-Liposome suspension was almost completely encapsulated in the liposome bilayer, preventing the hydrolysis reaction in the Rubropunctatin molecule under alkaline conditions. Thus, R-Liposome improves the pH stability of Rubropunctatin.

In order to further explore whether Rubropunctatin was hydrolyzed under strong alkaline conditions, the reaction of Rubropunctatin in a KOH solution at pH 12.0 was investigated by ion-trap LC/MS. The mass spectrometry data is presented in Fig. 4A, indicating that when the liquid chromatographic peak time is in a range from 3 to 11 min (not shown), the molecular weight of the main substance is 372, which is 18 more than that of Rubropunctatin. At this point, the carboxylic acid is formed by hydrolysis of the Rubropunctatin lactone (Fig. 4B, I) or a carboxylate (Fig. 4B, II), 373.1647 is a carboxylic acid plus H peak, and 411.1204 is a carboxylate plus H peak. Thus, Rubropunctatin was hydrolyzed under strong alkaline conditions, and R-Liposome almost completely embedded Rubropunctatin in the bilayer of the liposome, which greatly improved the pH stability of Rubropunctatin.

3.3 Photostability

Rubropunctatin is prone to photochemical reaction under light conditions and is gradually degraded, which limits its application in actual production and use in life. However, encapsulation systems such as β-CDs or liposomes provide a molecular shield for photolabile drugs, thereby delaying their

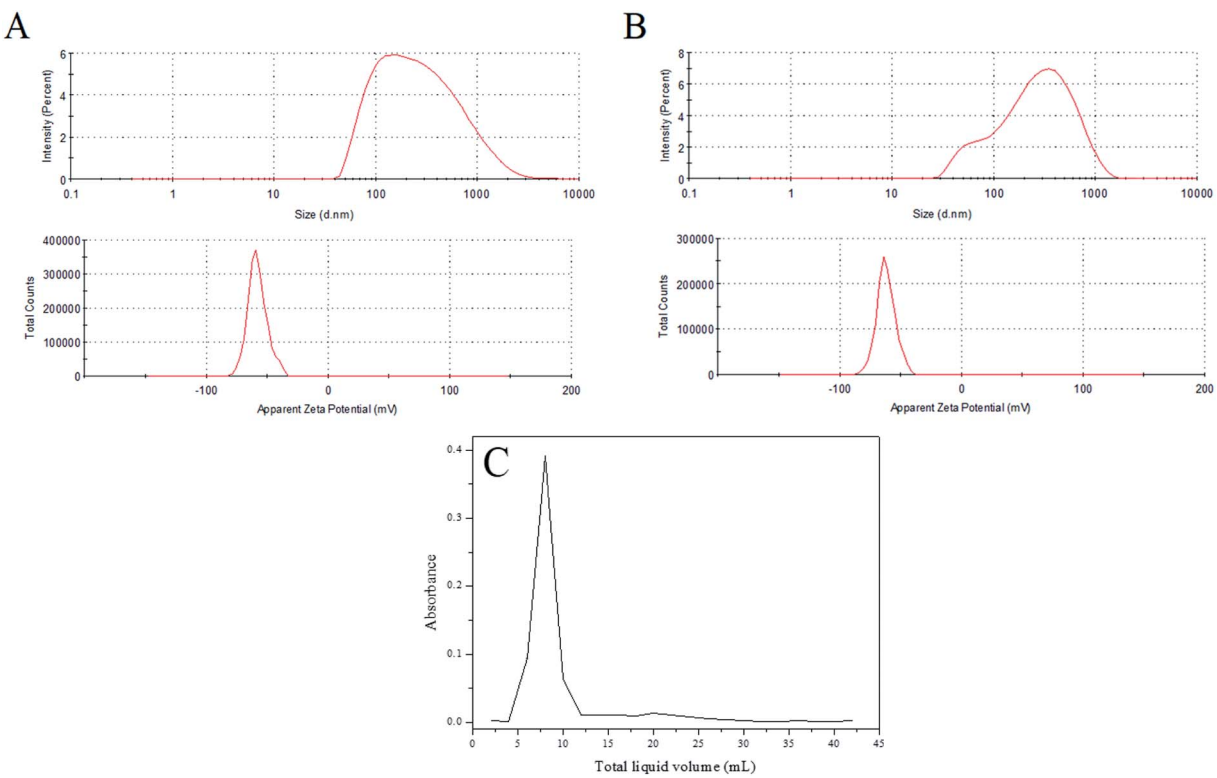

Fig. 2 Distribution of particle size and zeta potential: (A) blank liposome; (B) R-Liposome; (C) the elution curve of the R-Liposome suspension agent.

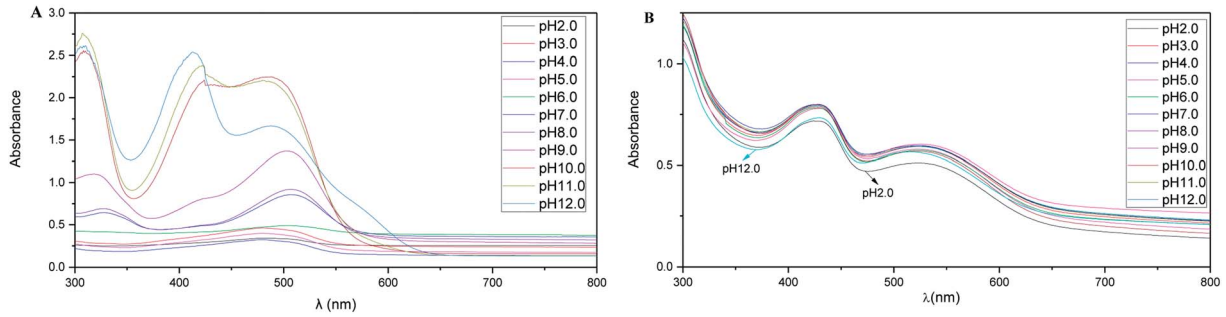

Fig. 3 UV-vis spectra of the Rubropunctatin solution (A) and R-Liposome suspension (B) under different pH conditions dissolved in absolute ethanol.

photodegradation.[35,36] Therefore, our study compared and analyzed the photostability of Rubropunctatin on its own and with R-Liposome.

As shown in Fig. 5, after 2 h of irradiation, Rubropunctatin alone reduced rapidly (about 77%), nevertheless 70.03 ± 1.67% of Rubropunctatin remained in the R-Liposome. Moreover, after 4 h, approximately 60% of Rubropunctatin still remained in the suspension of R-Liposome, indicating that the encapsulation system with a liposome improved the photostability of Rubropunctatin, so that after Rubropunctatin was encapsulated in lipids, the photodegradation of Rubropunctatin can be prevented. The rapid decrease in the preservation rate of Rubropunctatin with R-Liposome within 2 h may be caused by the degradation of Rubropunctatin that is not completely encapsulated in the liposome.

3.4 *In vitro* release

One of the most important criteria to be considered in food applications is the release from carriers. The action of the active

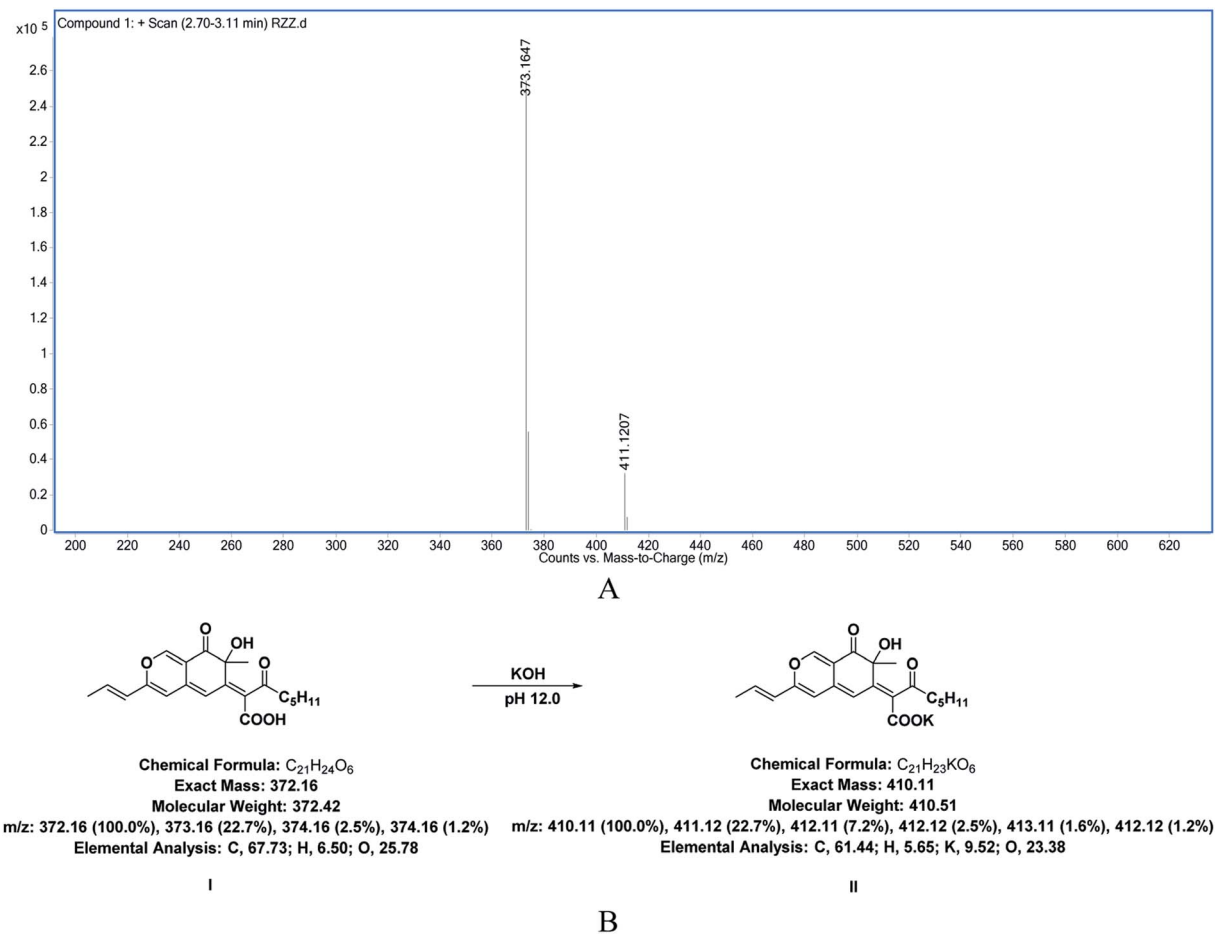

Fig. 4 (A) Mass spectrometry results and (B) molecular structure diagrams of the hydrolysate of Rubropunctatin in KOH solution at pH 12.0.

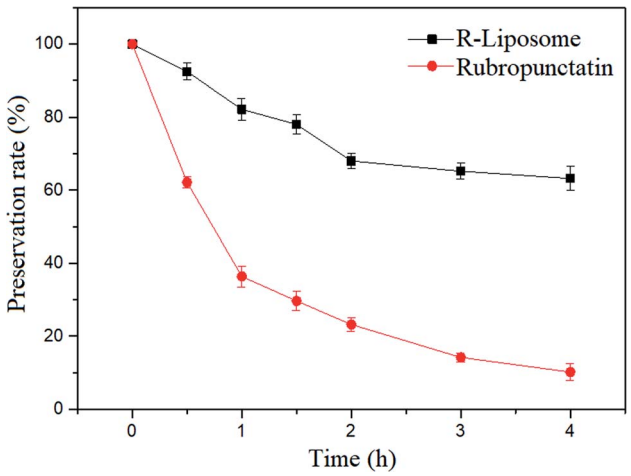

Fig. 5 The percentage of Rubropunctatin remaining in the solution as a function of time (light source: tungsten halogen lamp, 500 W, wavelength: 597–622 nm).

compounds and their effects will be maintained by extending their release.[37]

The release profile of free Rubropunctatin and R-Liposome suspensions were evaluated. According to Fig. 6, Rubropunctatin and R-Liposome were both rapidly released in the first 7 h (first phase), followed by a relatively mild release over the next 48 h (second phase). The release rate tended to be stable over time. In comparison, the release rate of R-Liposome is approximately 40% lower than that of free Rubropunctatin during the first 7 h. Moreover, the calculated cumulative percentage of free Rubropunctatin was 97 ± 1.15% at 48 h. However, R-Liposome showed a better sustained-release property. For R-Liposome, the first phase of release may be caused by the release of Rubropunctatin incorporated in the external monolayer of the membrane; while Rubropunctatin embedded in the internal phospholipid bilayer may be released in the second phase. At the same time, it is worth noting that the *in vitro* release profile of free Rubropunctatin also showed a relatively weak sustained release effect, because free Rubropunctatin is completely water-insensitive, so the sample needs to be dissolved in 0.4% DMSO to obtain free Rubropunctatin.

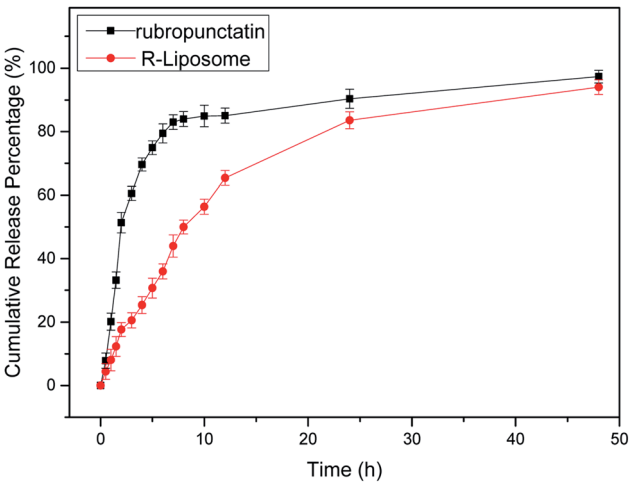

Fig. 6 *In vitro* cumulative release properties of the R-Liposome suspension.

It can be inferred that since Rubropunctatin was encapsulated in a hydrophobic core, it was slowly degraded. The slow release behavior from the liposome might be useful in keeping Rubropunctatin in the liposome and in the gastrointestinal tract, leading to an increase in its oral absorption and thus oral bioavailability.

3.5 MTT assay

According to our previous study, we found that Rubropunctatin possessed higher anticancer activity and less cytotoxicity than taxol for the normal gastric epithelial cells.[17] In this work, we evaluated the cytotoxic activity of R-Liposome on HeLa cells.

The experimental results are shown in Fig. 7. As shown in Fig. 7A, morphological changes in the cells under different drug concentrations were observed by microscope. It can be seen that the morphology of the blank control group shows irregular polygons and the number of normal morphological cells and cells in an abnormal state, such as following deflation and floating, gradually decreased and increased, respectively, indicating that the inhibition of cell proliferation of R-Liposome is dose-dependent.

It is worth noting that free Rubropunctatin has no cytotoxicity due to its water insolubility (Fig. 7B). However, Rubropunctatin, solubilized in 0.4% DMSO and encapsulated in a liposome, has a significant toxic effect in HeLa cells in a dose-dependent manner. The IC_{50} values were 26.60 ± 0.64 μmol L^{-1} (Rubropunctatin, solubilized in 0.4% DMSO) and 64.312 ± 1.16 μmol L^{-1} (Rubropunctatin, encapsulated in the liposome), respectively. Thus, that of R-Liposome was lower than Rubropunctatin solubilized in 0.4% DMSO. It is worth mentioning that R-Liposome has greater cell inhibition than Rubropunctatin dissolved in 0.4% DMSO at the same concentration of 100 μM. This result might be due to the slow release of R-Liposome.

In conclusion, pure Rubropunctatin has no anticancer activity and DMSO cannot be used during *in vivo* experiments, so in order to improve its anticancer activity, the encapsulation of Rubropunctatin in a liposome proved necessary.

3.6 Cell apoptosis

In this work, Annexin-V-FITC/PI double staining was used to quantitatively determine the apoptosis-inducing effect of R-Liposome. Fig. 8B shows the increasing proportion of cells in the apoptotic phase with increasing drug concentration. As shown in Fig. 8A, the normal cells of the blank control group accounted for 98.7%. The addition of the R-Liposome suspension resulted in apoptosis of cells. After 10 μmol L^{-1} suspension was added to the HeLa cells for 24 h, the number of normal cells accounted for 40.2% of the total cells, and 59.5% of the cells were in the apoptotic phase (including early apoptosis and late apoptotic cells). The results indicated that with the increase of the concentration of the R-Liposome suspension, the

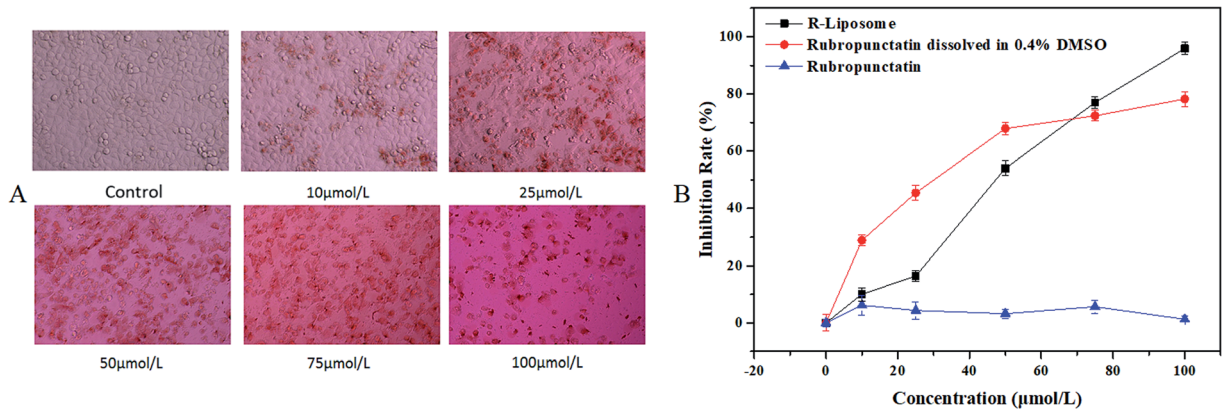

Fig. 7 (A) Morphological observation (×40); (B) growth inhibition curve of HeLa cells treated with different concentrations of the R-Liposome suspension.

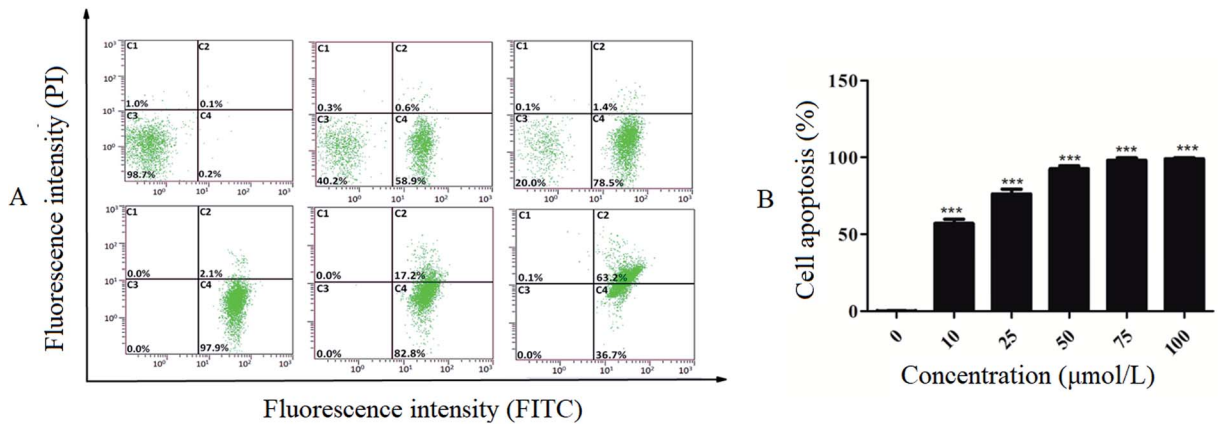

Fig. 8 Induction of apoptosis in HeLa cells (C1: dead cells; C2: late apoptotic/necrotic cells; C3: non-apoptotic cells; C4: early apoptotic cells). The dosing concentration from left to right, and from above to bottom is 0, 10, 25, 50, 75, and 100 μmol L^{-1}. (A) Fluorescence map and (B) fluorometric quantification of the apoptosis of the cells.

proportion of cells in the late stage of the apoptosis phase significantly increased.

Furthermore, when the concentration was 50 μmol L^{-1}, all of the cells were in the apoptotic phase, and 97.9% of the cells were in the early stage of apoptosis. The proportion of late apoptotic cells significantly increased as the concentration of the R-Liposome suspension increased. The experimental results indicate that the R-Liposome suspension can induce apoptosis of HeLa cells. There is one possible explanation for this observation. Liposomes have great biocompatibility properties and high affinity with cell membranes, so Rubropunctatin encapsulated in a liposome is more likely to combine with cell membranes, resulting in cell membrane surface damage and cell inner membrane eversion, thereby inducing cell apoptosis.

4. Conclusion

In this study, we have successfully developed a novel formulation of R-Liposome by a film dispersion method, and Rubropunctatin was successfully encapsulated into a liposome. The results clearly showed that the R-Liposome we built was small in size and the encapsulation of Rubropunctatin could be achieved with high entrapment efficiency, and this greatly enhanced its water solubility and stability. Moreover, R-Liposome protected Rubropunctatin from photodegradation. The *in vitro* release profile indicated that the R-Liposome suspension exhibited sustained slow release behavior. In the *in vitro* cell assay, the R-Liposomes showed a clear anticancer advantage over free Rubropunctatin. This finding emphasizes a potential application of liposomal nanoparticles as drug delivery vehicles of Rubropunctatin for the treatment of cancers. Further work will be needed to study the anticancer efficacy *in vivo* of R-Liposome and to decorate the liposome for wide clinical applications in the treatment of cancers.

Conflicts of interest

The authors report no conflicts of interest. The authors alone are responsible for the content and writing of this article.

Acknowledgements

This work was supported by the Natural Science Foundation of Fujian Province of China (No. 2017J01854), the Fujian Province Young and Middle-aged Teacher Education Research Project (JAT160655), and the Marine High-tech Industry Development Special Project of Fujian Province of China (Min Marine High-tech [2015]01).

References

1 Y. L. Lin, T. H. Wang, M. H. Lee and N. W. Su, *Appl. Microbiol. Biotechnol.*, 2008, **77**, 965–973.
2 Y. Qian, X. Liang, J. Yang, C. Zhao, W. Nie, L. Liu, T. Yi, Y. Jiang, J. Geng, X. Zhao and X. Wei, *ACS Appl. Mater. Interfaces*, 2018, **10**, 32006–32016.
3 K. Yasukawa, M. Takahashi, S. Natori, K. Kawai, M. Yamazaki, M. Takeuchi and M. Takido, *Oncology*, 1994, **51**, 108–112.
4 T. Akihisa, H. Tokuda, K. Yasukawa, M. Ukiya, A. Kiyota, N. Sakamoto, T. Suzuki, N. Tanabe and H. Nishino, *J. Agric. Food Chem.*, 2005, **53**, 562–565.
5 N. W. Su, Y. L. Lin, M. H. Lee and C. Y. Ho, *J. Agric. Food Chem.*, 2005, **53**, 1949–1954.
6 B. Y. Ho and T. M. Pan, *J. Agric. Food Chem.*, 2009, **57**, 8258–8265.
7 N. Osmanova, W. Schultze and N. Ayoub, *Phytochem. Rev.*, 2010, **9**, 315–342.
8 M. Y. Hong, N. P. Seeram, Y. Zhang and D. Heber, *J. Nutr. Biochem.*, 2008, **19**, 448–458.
9 Y. Yang, B. Liu, X. L. Du, P. Li, B. Liang, X. Z. Cheng, L. C. Du, D. Huang, L. Wang and S. Wang, *Sci. Rep.*, 2015, **5**, 8331–8339.
10 R. M. Schweiggert, *J. Agric. Food Chem.*, 2018, **66**, 3074–3081.
11 W. P. Chen, Y. L. Feng, I. Molnar and F. S. Chen, *Nat. Prod. Rep.*, 2019, **36**, 561–572.
12 K. Tai, M. Rappolt, X. He, Y. Wei, S. Zhu, J. Zhang, L. Mao, Y. Gao and F. Yuan, *Food Chem.*, 2019, **293**, 92–102.
13 J. Wan, D. Li, R. Song, B. R. Shah, B. Li and Y. Li, *Food Chem.*, 2017, **221**, 760–770.
14 J. M. Gao, S. X. Yang and J. C. Qin, *Chem. Rev.*, 2013, **113**, 4755–4811.
15 Y. Q. Zheng, Y. Zhang, D. S. Chen, H. J. Chen, L. Lin, C. Z. Zheng and Y. H. Guo, *J. Agric. Food Chem.*, 2016, **64**, 2541–2548.
16 H. L. Tan, Z. Y. Xing, G. Chen, X. F. Tian and Z. Q. Wu, *Molecules*, 2018, **23**, 3242–3252.
17 Y. Q. Zheng, Y. W. Xin, X. A. Shi and Y. H. Guo, *J. Agric. Food Chem.*, 2010, **58**, 9523–9528.
18 Z. Z. Ren, Y. N. Xu, Z. X. Lu, Z. Z. Wang, C. Q. Chen, Y. H. Guo, X. A. Shi, F. Li, J. M. Yang and Y. Q. Zheng, *RSC Adv.*, 2019, **9**, 11396–11405.
19 K. Krukiewicz and J. K. Zak, *Mater. Sci. Eng., C*, 2016, **62**, 927–942.
20 A. K. Sharma, A. Gothwal, P. Kesharwani, H. Alsaab, A. K. Iyer and U. Gupta, *Drug Discovery Today*, 2017, **22**, 314–326.
21 S. Zununi Vahed, R. Salehi, S. Davaran and S. Sharifi, *Mater. Sci. Eng., C*, 2017, **71**, 1327–1341.
22 C. Jaafar-Maalej, R. Diab, V. Andrieu, A. Elaissari and H. Fessi, *J. Liposome Res.*, 2010, **20**, 228–243.
23 J. S. Lee, J. W. Suh, E. S. Kim and H. G. Lee, *J. Agric. Food Chem.*, 2017, **65**, 8930–8937.
24 M. Watanabe, K. Kawano, K. Toma, Y. Hattori and Y. Maitani, *J. Controlled Release*, 2008, **127**, 231–238.
25 Y. Fan and Q. Zhang, *Asian J. Pharm. Sci.*, 2013, **8**, 81–87.
26 Y. Niu, X. Wang, S. Chai, Z. Chen, X. An and W. Shen, *J. Agric. Food Chem.*, 2012, **60**, 1865–1870.
27 A. P. Ranjan, A. Mukerjee, L. Helson, R. Gupta and J. K. Wishwanatha, *Anticancer Res.*, 2013, **33**, 3603–3610.
28 G. Yang, T. Yang, W. Zhang, M. Lu, X. Ma and G. Xiang, *J. Agric. Food Chem.*, 2014, **62**, 2207–2215.
29 X. Song, Y. Zhao, W. Wu, Y. Bi, Z. Cai, Q. Chen, Y. Li and S. Hou, *Int. J. Pharm.*, 2008, **350**, 320–329.
30 J. S. N. Anjali Pant, *Eur. J. Pharm. Sci.*, 2018, **112**, 180–185.
31 Y. Chen, Q. Wu, Z. Zhang, L. Yuan, X. Liu and L. Zhou, *Molecules*, 2012, **17**, 5972–5987.
32 Y. Chen, Q. Wu, Z. Zhang, L. Yuan, X. Liu and L. Zhou, *Molecules*, 2012, **17**, 5972–5987.
33 C. Mohanty and S. K. Sahoo, *Biomaterials*, 2010, **31**, 6597–6611.
34 H. Zhang, L. Shen, G. Xu and Y. Chen, *Shipin Yu Fajiao Gongye*, 2008, **31**, 129–133.
35 M. Najlah, A. Said Suliman, I. Tolaymat, S. Kurusamy, V. Kannappan, A. M. A. Elhissi and W. Wang, *Pharmaceutics*, 2019, **11**, 610–611.
36 Y. Y. Jiao, X. Q. Wang, W. L. Lu, Z. J. Yang and Q. Zhang, *Eur. J. Pharm. Sci.*, 2013, **48**, 249–258.
37 J. Rodríguez, M. J. Martín, M. A. Ruiz and B. Clares, *Food Res. Int.*, 2016, **83**, 41–59.

